Width of the Confining String in Yang-Mills Theory

F. Gliozzi,[1] M. Pepe,[2] and U.-J. Wiese[3]

[1]Dipartimento di Fisica Teorica, Università di Torino, and INFN, Sezione di Torino, via P. Giuria 1, 10125 Torino, Italy
[2]INFN, Sezione di Milano-Bicocca, Edificio U2, Piazza della Scienza 3, 20126 Milano, Italy
[3]Albert Einstein Center for Fundamental Physics, Institute for Theoretical Physics, Bern University, Sidlerstrasse 5, 3012 Bern, Switzerland

(Received 11 March 2010; published 8 June 2010)

We investigate the transverse fluctuations of the confining string connecting two static quarks in $(2+1)$D $SU(2)$ Yang-Mills theory using Monte Carlo calculations. The exponentially suppressed signal is extracted from the large noise by a very efficient multilevel algorithm. The resulting width of the string increases logarithmically with the distance between the static quark charges. Corrections at intermediate distances due to universal higher-order terms in the effective string action are calculated analytically. They accurately fit the numerical data.

DOI: 10.1103/PhysRevLett.104.232001 PACS numbers: 12.38.Gc, 11.15.Ha, 12.38.Aw, 12.38.Lg

Understanding the dynamics of confining strings connecting static quarks and antiquarks in non-Abelian gauge theories is a great challenge in strong interaction physics. During its time evolution, a confining string sweeps out a world sheet whose boundary is determined by the world lines of the static external quark charges. The string world sheet can also be viewed as an analog of a fluctuating interface separating different phases of condensed matter. Just like a rough interface, the confining string in a non-Abelian gauge theory supports massless transverse fluctuations. Interestingly, the dynamics of these fluctuations—known as capillary waves in condensed matter physics—is captured by a systematic two-dimensional low-energy effective field theory. In the effective theory, the string is described by a $(d-2)$-component vector $\vec{h}(x,t)$ pointing to the location of the string world sheet in the $(d-2)$ transverse dimensions of a d-dimensional space-time. Here $x \in [0, r]$ and $t \in [0, \beta]$ are the Euclidean coordinates parametrizing the base space, with r being the fixed distance between the external static charges and the inverse temperature β being the extent of Euclidean time. Since the string ends at the static quark charges, its fluctuation field obeys the boundary condition $\vec{h}(0,t) = \vec{h}(r,t) = \vec{0}$. The leading term in the action of the effective theory

$$S[\vec{h}] = \frac{\sigma}{2} \int_0^\beta dt \int_0^r dx\, \partial_\mu \vec{h} \cdot \partial_\mu \vec{h}, \qquad \mu \in \{1,2\}, \quad (1)$$

gives rise to a universal contribution to the static quark potential

$$V(r) = \sigma r - \frac{\pi(d-2)}{24r} + \mathcal{O}(1/r^3), \quad (2)$$

where σ is the string tension. The universal Lüscher term is proportional to the number $(d-2)$ of transverse directions in which the string is fluctuating [1,2]. The effective action from above also accounts for the string width [3]. Because of its transverse fluctuations, the string broadens as the quark sources are separated. More precisely the transverse area swept out by the flux tube increases logarithmically with separation. At the distance $r/2$ halfway between the external static quark sources, at leading order the string has the squared width

$$w_{\rm lo}^2(r/2) = \frac{d-2}{2\pi\sigma} \log\left(\frac{r}{r_0}\right), \quad (3)$$

where r_0 is some distance scale. This fundamental formula for the width is again universal. It applies to strings in confining gauge theories, to fundamental strings, as well as to fluctuating interfaces in condensed matter physics. Interestingly, until now the logarithmic behavior of the string width has been verified only in the context of spin models. Below the critical temperature of the 3D Ising model, but above the corresponding roughening transition, an interface separating the broken phases indeed has massless fluctuations described by the effective theory of Eq. (1). Using an efficient cluster algorithm, the expression for the width of Eq. (3) has been verified in [4]. By a duality transformation, the results obtained in the 3D Ising model also apply to $(2+1)$D Abelian $\mathbb{Z}(2)$ lattice gauge theory, where the effective theory has been confirmed in more detail also using different boundary conditions [5]. Similar results have been obtained in a $(2+1)$D $\mathbb{Z}(4)$ gauge theory [6]. In non-Abelian gauge theories the measurement of the string width is computationally very challenging; early calculations were affected by large statistical errors and did thus not lead to definite conclusions [7].

In this Letter, for the first time we verify the logarithmically divergent string width for a non-Abelian gauge theory by simulating $(2+1)$D $SU(2)$ lattice Yang-Mills theory using a very efficient multilevel algorithm [8,9]. As we will see, the Monte Carlo data agree with the analytic prediction at large distances r. Before we turn to the numerical results, we systematically work out corrections at intermediate distances, which arise due to higher-order terms in

the low-energy effective action. For $d = 3$ there is only one transverse dimension, and hence in this case $h(x, t) \in \mathbb{R}$ is a one-component scalar field. The leading and next-to-leading terms in the low-energy effective action describing the massless transverse fluctuations of the string are then given by

$$S[h] = \frac{\sigma}{2} \int_0^\beta dt \int_0^r dx \left[\partial_\mu h \partial_\mu h - \frac{1}{4} (\partial_\mu h \partial_\mu h)^2 \right]. \quad (4)$$

Since the Dirichlet boundary conditions $h(0, t) = h(r, t) = 0$ explicitly break translation invariance, one may have expected boundary terms to be present in the effective action as well [9]. Remarkably, due to open-closed string duality, such terms are absent and the prefactor of the first subleading term is uniquely determined [10]. A generalization of these arguments shows that for $d = 3$ there is only one six-derivative term which coincides with the one of the Nambu-Goto action [11].

The effective action of Eq. (4) describes string fluctuations in the continuum. Before one reaches the continuum limit, the confining string in a lattice Yang-Mills theory is also affected by lattice artifacts. First of all, at very strong coupling the world sheet swept out by the lattice string is rigid, i.e., it follows the discrete lattice steps and does not even have massless excitations. Only at weaker coupling, after crossing the roughening transition, the string world sheet supports massless excitations and thus becomes rough. Consequently, the effective theory is applicable only in the rough phase.

For a string world sheet with periodic boundary conditions in Euclidean time, the squared width of the string is given by

$$w^2(x) = \langle h(x, t)^2 \rangle, \quad (5)$$

which is directly related to the two-point function $\langle h(x, t) h(x', t') \rangle$, with the two points (x, t) and (x', t') falling on top of each other. This limit leads to ultraviolet divergences which we regularize using the point-splitting procedure

$$\langle h(x, t)^2 \rangle \to \langle h(x, t) h(x' = x + \epsilon, t' = t + \epsilon') \rangle. \quad (6)$$

At the end, one sets $\epsilon \to 0$, $\epsilon' \to 0$ and the remaining ultraviolet divergent terms are absorbed in physical length scales. In the leading order Gaussian approximation of Eq. (1), the two-point function can be conveniently expressed in the form

$$\langle h(x, t) h(x', t') \rangle = \frac{1}{\pi\sigma} \sum_{n=1}^{\infty} \sin n\xi_1 \sin n\xi_1' \frac{e^{-n\xi_2} + q^n e^{n\xi_2}}{n(1 - q^n)}, \quad (7)$$

where $\xi_1 = \pi x/r$, $\xi_1' = \pi x'/r$, $\xi_2 = \pi(t - t')/r$ with $0 \le \xi_2 \le \pi\beta/r$. The parameter $q = e^{2\pi i \tau}$ depends on the ratio $\tau = i\beta/(2r)$. One then obtains the squared width of the string as

$$w_{\rm lo}^2(r/2) = \frac{1}{2\pi\sigma} \log\left(\frac{r}{r_0}\right) + \frac{1}{\pi\sigma} \log\left(\frac{\eta(2\tau)}{\eta(\tau)^2}\right), \quad (8)$$

with $r_0 = \pi|\epsilon + i\epsilon'|/2$ and the Dedekind function

$$\eta(\tau) = q^{1/24} \prod_{n=1}^{\infty} (1 - q^n). \quad (9)$$

In the numerical simulations we put $r \ll \beta$. Then there are only exponentially small corrections to the logarithmic broadening of the width of the string. On the other hand, for $r \gg \beta$, the inversion transformation property

$$\eta(\tau) = \eta(-1/\tau)/\sqrt{-i\tau} \quad (10)$$

implies that

$$w_{\rm lo}^2(r/2) = \frac{1}{2\pi\sigma} \log\left(\frac{\beta}{4r_0}\right) + \frac{r}{4\beta\sigma} + \mathcal{O}(e^{-2\pi r/\beta}). \quad (11)$$

This shows that, at finite temperature, the confining string broadens linearly with the distance between the external static quarks [12].

The non-Gaussian correction due to the first subleading term in Eq. (4) results from the six-point function

$$\frac{\sigma}{8} \left\langle h\left(\frac{r}{2}, 0\right) h\left(\frac{r}{2} + \epsilon, \epsilon'\right) \left[\int_0^r dx \int_0^\beta dt (\partial_\mu h \partial_\mu h)^2 \right] \right\rangle. \quad (12)$$

This amplitude has two kinds of ultraviolet divergent terms: one proportional to $\log|\epsilon + i\epsilon'|$ and the other proportional to $(\epsilon^2 - \epsilon'^2)/|\epsilon + i\epsilon'|^4$. The former is absorbed in the scale of the logarithm and the latter is eliminated by putting $\epsilon^2 = \epsilon'^2$. Therefore the contribution to w^2 of the next-to-leading term does not require the introduction of new low-energy parameters. Up to first order in the expansion parameter $1/(\sigma r^2)$, the complete expression turns out to be

$$\begin{aligned} w^2(r/2) &= \left(1 + \frac{4\pi f(\tau)}{\sigma r^2}\right) w_{\rm lo}^2(r/2) - \frac{f(\tau) + g(\tau)}{\sigma^2 r^2}, \\ f(\tau) &= \frac{E_2(\tau) - 4E_2(2\tau)}{48}, \\ g(\tau) &= i\pi\tau \left(\frac{E_2(\tau)}{12} - q\frac{d}{dq}\right)\left(f(\tau) + \frac{E_2(\tau)}{16}\right) + \frac{E_2(\tau)}{96}, \\ E_2(\tau) &= 1 - 24 \sum_{n=1}^{\infty} \frac{nq^n}{1 - q^n}. \end{aligned} \quad (13)$$

Here $E_2(\tau)$ is the first Eisenstein series. Just like the action, the operator $h(x, t)$ also receives higher-order corrections. Remarkably, their effect vanishes in Eq. (13). The derivation of these results will be presented in [13].

Lattice gauge theory is a powerful tool that allows us to address the question of string dynamics from first principles. Since it is least problematical for numerical simulations, we consider (2 + 1)D $SU(2)$ Yang-Mills theory on a cubic lattice of size $L \times L \times \beta$, with the Euclidean time extent β determining the inverse temperature. We use the standard Wilson plaquette action

$$S[U] = -\frac{2}{g^2}\sum_{x,\mu,\nu}\mathrm{Tr}[U_{x,\mu}U_{x+\hat{\mu},\nu}U^{\dagger}_{x+\hat{\nu},\mu}U^{\dagger}_{x,\nu}], \qquad (14)$$

for parallel transporter variables $U_{x,\mu} \in SU(2)$ in the fundamental representation of the gauge group, located on the links (x, μ). Here g is the bare gauge coupling and $\hat{\mu}$ is a unit-vector pointing in the μ direction. It should be noted that all physical quantities are measured in units of the lattice spacing which we put to 1. The partition function takes the form

$$Z = \int \mathcal{D}U e^{-S[U]} = \prod_{x,\mu}\int_{SU(2)} dU_{x,\mu} e^{-S[U]}, \qquad (15)$$

where $dU_{x,\mu}$ denotes the local gauge invariant Haar measure on the link (x, μ). An external static quark located at the site x is represented by a Polyakov loop

$$\Phi_x = \frac{1}{2}\mathrm{Tr}\Big[\prod_{t=1}^{\beta} U_{x+t\hat{2},2}\Big], \qquad (16)$$

a parallel transporter wrapping around the periodic Euclidean time direction. We have chosen the 2 direction to represent Euclidean time. When two external quark charges are separated along the 1 direction, the world sheet of the confining string extends in the space-time directions $\mu = 1, 2$, while the string fluctuates in the transverse 3 direction. The static quark potential $V(r)$ results from the Polyakov loop correlation function

$$\langle\Phi_0\Phi_r\rangle = \frac{1}{Z}\int \mathcal{D}U\Phi_0\Phi_r e^{-S[U]} \sim e^{-\beta V(r)}, \qquad (17)$$

in the zero-temperature limit $\beta \to \infty$.

In order to ensure a good projection on the ground state of the string and in order to cover a wide range of spatial distances satisfying $r < \beta$, we have simulated at inverse temperatures as large as $\beta = 48$ in lattice units. The spatial lattice size was $L = 54$ and the bare gauge coupling was chosen as $4/g^2 = 9.0$ which puts the deconfinement phase transition at $\beta_c \approx 6$. The numerical simulations have been performed using the Lüscher-Weisz technique [8,9] with two levels. We measure the static potential using the Polyakov loop two-point function and we obtain $\sigma = 0.025\,897(15)$ for the string tension: this result is compatible with the value reported in [14].

The width of the fluctuating string is obtained from the connected correlation function

$$C(x_3) = \frac{\langle\Phi_0\Phi_r P_x\rangle}{\langle\Phi_0\Phi_r\rangle} - \langle P_x\rangle, \qquad (18)$$

of a pair of Polyakov loops with a single plaquette

$$P_x = \frac{1}{2}\mathrm{Tr}[U_{x,1}U_{x+\hat{1},2}U^{\dagger}_{x+\hat{2},1}U^{\dagger}_{x,2}], \qquad (19)$$

in the 1-2 plane, which measures the color-electric field along the 1 direction of the string as a function of the transverse displacement x_3. The plaquette is located at the site $x = (r/2, 0, x_3)$ and thus measures the transverse fluctuations of the color flux tube at the maximal distance $r/2$ from the external quark charges. The correlation function at distance $r = 19$ is illustrated in Fig. 1. The data show the expected bell shape of a Gaussian distribution, but their high numerical accuracy also reveals small deviations. We fit the data using the ansatz

$$\frac{\langle\Phi_0\Phi_r P_x\rangle}{\langle\Phi_0\Phi_r\rangle} = A\exp(-x_3^2/T)\frac{1 + B\exp(-x_3^2/T)}{1 + D\exp(-x_3^2/T)} + K, \qquad (20)$$

where A, B, D, T, and K are fit parameters. This function always provides an excellent fit of the data. The squared width of the string is then obtained as the second moment of the correlation function

$$w^2(r/2) = \frac{\int dx_3\, x_3^2 C(x_3)}{\int dx_3\, C(x_3)}. \qquad (21)$$

In order to check the dependence of the measured string width on the ansatz of Eq. (20), we have also considered other fit functions. As long as the ansatz provided a very good fit of the numerical data, we have not observed a significant effect on the measured string width. Hence, systematic uncertainties due to the fitting ansatz were negligible compared to the statistical errors. In Fig. 2 we illustrate the dependence of the squared string width $w^2(r/2)$ on the distance r between the external static quarks. At distances larger than $r \approx 18$, the Monte Carlo data are well represented by the effective field theory prediction of Eq. (13). In particular, the predicted prefactor $1/(2\pi\sigma)$ of the logarithmic term $\log(r/r_0)$ is confirmed by the numerical data. It should be noted that the string tension has already been determined by the fit to the static quark potential. The only free parameter in the fit of the Monte Carlo data for the width is the scale r_0: we obtain $r_0 = 2.26(2)$ such that $r_0\sqrt{\sigma} = 0.364(3)$.

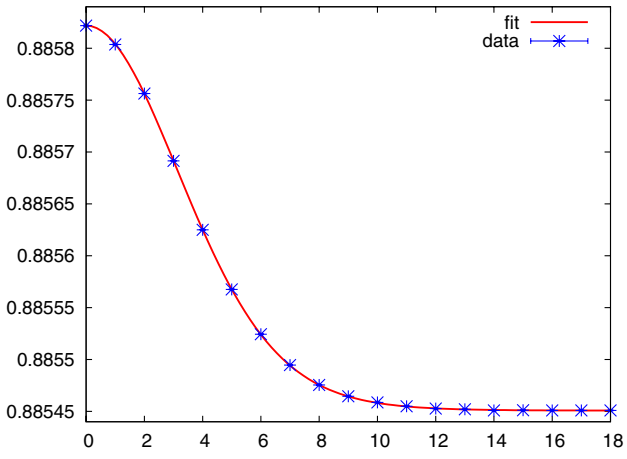

FIG. 1 (color online). The ratio $\langle\Phi_0\Phi_r P_x\rangle/\langle\Phi_0\Phi_r\rangle$ as a function of the transverse displacement x_3 at fixed distance $r = 19$ between the external static quarks. The solid line is a fit of the numerical data using Eq. (20).

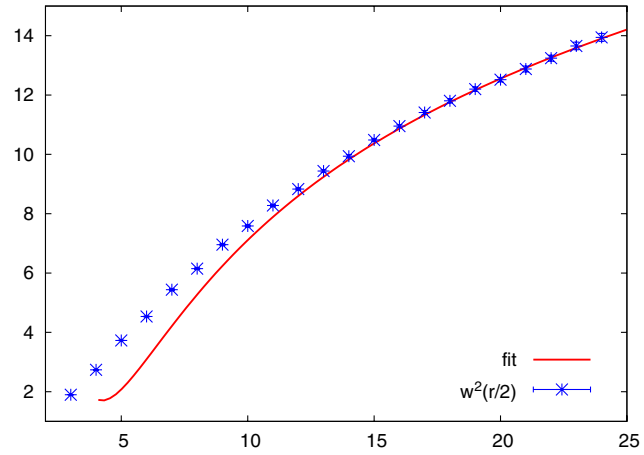

FIG. 2 (color online). The squared width of the confining string $w^2(r/2)$ at its midpoint as a function of the distance r between the external quark charges. The solid curve is a fit to the next-to-leading order prediction of the low-energy effective field theory from Eq. (13).

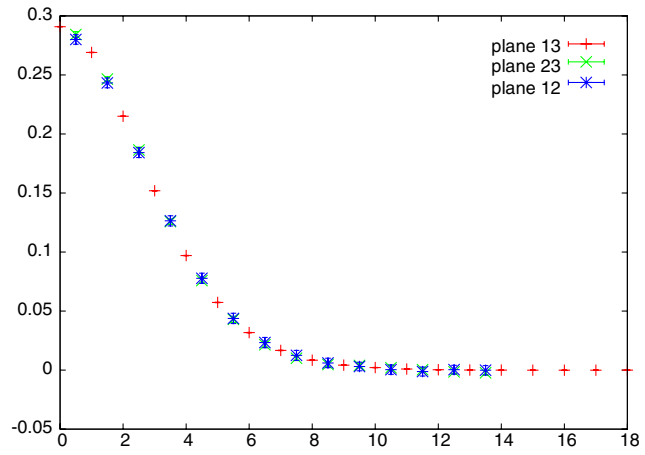

FIG. 3 (color online). Probability distribution $C(x_3)/\int dx_3 C(x_3)$ using the three possible orientations of the plaquette in Eq. (18). The data points for the two orientations orthogonal to the string world sheet are put at the midpoint between two lattice sites.

It should be noted that the effective theory prediction of Eq. (13) does not include lattice artifacts due to the violation of rotation invariance. Since the lattice theory is invariant only under discrete rotations and not under the full Poincaré group, before one reaches the continuum limit the two additional terms $\sum_{\mu=1,2}(\partial_\mu \partial_\mu h)^2$ and $\sum_{\mu=1,2}(\partial_\mu h)^4$ enter the effective theory. Since these terms contain four derivatives, they are of next-to-leading order. Hence, they have no effect on the Lüscher term or on the leading logarithmic behavior of the string width. The corrections due to the rotation symmetry breaking terms can be computed [13] and included in the fit for the string width. This adds two free parameters and makes the fit excellent down to $r \approx 10$. However, an approximate estimate of the correction to the string width coming from the rotation invariant next-to-next-to-leading order may also significantly improve the agreement in the range $r = 10$–18. Since, at the moment, we cannot clearly disentangle these two effects, we have not taken into account rotation symmetry breaking corrections in our data analysis.

In the numerical results discussed so far, the plaquette orientation was parallel to the string world sheet. The plaquette acts as a probe that measures the fluctuations of the confining string. The width depends on the probe through the value of the low-energy parameter r_0. Choosing different probes—and thus different ways of defining the string width—we expect, however, only small changes in the value of the low-energy parameter r_0. In order to investigate this issue, we have considered different orientations of the plaquette in the definition of Eq. (18). In Fig. 3 we show the normalized probability distribution $C(x_3)/\int dx_3 C(x_3)$ for the 3 different orientations of the plaquette at fixed distance $r = 12$ between the external static quarks. The numerical data show that the normalized probability distribution is not significantly affected by the different probes used to extract the color flux tube width. Early investigations in 4D can be found in [15].

We gratefully acknowledge helpful discussions with M. Caselle, P. Hasenfratz, F. Niedermayer, R. Sommer, and P. Weisz. This work is supported in part by funds provided by the Schweizerischer Nationalfonds (SNF). The computations reported in this Letter have been partially performed on the cluster Lagrange at CILEA.

[1] M. Lüscher, K. Symanzik, and P. Weisz, Nucl. Phys. **B173**, 365 (1980).
[2] M. Lüscher, Nucl. Phys. **B180**, 317 (1981).
[3] M. Lüscher, G. Münster, and P. Weisz, Nucl. Phys. **B180**, 1 (1981).
[4] M. Hasenbusch and K. Pinn, Physica (Amsterdam) **192A**, 342 (1993).
[5] M. Caselle, F. Gliozzi, U. Magnea, and S. Vinti, Nucl. Phys. **B460**, 397 (1996).
[6] P. Giudice, F. Gliozzi, and S. Lottini, J. High Energy Phys. 01 (2007) 084.
[7] G. S. Bali, C. Schlichter, and K. Schilling, Phys. Rev. D **51**, 5165 (1995).
[8] M. Lüscher and P. Weisz, J. High Energy Phys. 09 (2001) 010.
[9] M. Lüscher and P. Weisz, J. High Energy Phys. 07 (2002) 049.
[10] M. Lüscher and P. Weisz, J. High Energy Phys. 07 (2004) 014.
[11] O. Aharony and E. Karzbrun, J. High Energy Phys. 06 (2009) 012.
[12] A. Allais and M. Caselle, J. High Energy Phys. 01 (2009) 073.
[13] F. Gliozzi, M. Pepe, and U.-J. Wiese (to be published).
[14] M. Caselle, M. Pepe, and A. Rago, J. High Energy Phys. 10 (2004) 005.
[15] R. Sommer, Nucl. Phys. **B306**, 181 (1988).